MOLECULAR ECOLOGY

Molecular Ecology (2017) doi: 10.1111/mec.14049

Specificity of root microbiomes in native-grown *Nicotiana attenuata* and plant responses to UVB increase *Deinococcus* colonization

RAKESH SANTHANAM,[1] YOUNGJOO OH,[1] RAMESH KUMAR,[1,2] ARNE WEINHOLD,[1] VAN THI LUU,[1] KARIN GROTEN[1] and IAN T. BALDWIN[1]

[1]*Department of Molecular Ecology, Max Planck Institute for Chemical Ecology, Hans-Knöll-Str. 8, Jena 07745, Germany,* [2]*CSIR – National Institute for Interdisciplinary Science and Technology (NIIST), Industrial Estate Po, Thiruvananthapuram, Kerala 695019, India*

Abstract

Plants recruit microbial communities from the soil in which they germinate. Our understanding of the recruitment process and the factors affecting it is still limited for most microbial taxa. We analysed several factors potentially affecting root microbiome structure – the importance of geographic location of natural populations, the microbiome of native seeds as putative source of colonization and the effect of a plant's response to UVB exposure on root colonization of highly abundant species. The microbiome of *Nicotiana attenuata* seeds was determined by a culture-dependent and culture-independent approach, and the root microbiome of natural *N. attenuata* populations from five different locations was analysed using 454-pyrosequencing. To specifically address the influence of UVB light on root colonization by *Deinococcus*, a genus abundant and consistently present in *N. attenuata* roots, transgenic lines impaired in UVB perception (ir*UVR8*) and response (ir*CHAL*) were investigated in a microcosm experiment with/without UVB supplementation using a synthetic bacterial community. The seed microbiome analysis indicated that *N. attenuata* seeds are sterile. Alpha and beta diversities of native root bacterial communities differed significantly between soil and root, while location had only a significant effect on the fungal but not the bacterial root communities. With UVB supplementation, root colonization of *Deinococcus* increased in wild type, but decreased in *irUVR8* and *irCHAL* plants compared to nontreated plants. Our results suggest that *N. attenuata* recruits a core root microbiome exclusively from soil, with fungal root colonization being less selective than bacterial colonization. Root colonization by *Deinococcus* depends on the plant's response to UVB.

Keywords: *Chalcone synthase*, *Deinococcus*, fungal and bacterial root colonization, microbiome, *Nicotiana attenuata*, pyrosequencing, UVB radiation, *UVR8*

Received 4 October 2016; revision received 24 January 2017; accepted 29 January 2017

Introduction

Soil is a highly heterogeneous ecosystem which harbours diverse communities of microbes. Plants, anchored in the soil by their roots, are colonized by diverse bacterial and fungal communities (Doornbos *et al.* 2011; Bulgarelli *et al.* 2012b; Hassan & Mathesius 2012; Hacquard *et al.* 2016). Different plant compartments (Bodenhausen *et al.* 2013; Santhanam *et al.* 2014; Fonseca-García *et al.* 2016; Coleman-Derr *et al.* 2016), and roots and soils harbour distinct microbial communities with root communities being less diverse than those of soil (Bulgarelli *et al.* 2012a).

The interaction among plants and microbes is well characterized for some partners, in particular for plant pathogens, plant growth-promoting bacteria and

Correspondence: Ian T. Baldwin and Karin Groten, Fax: +49 (0) 3641 571102; E-mails: baldwin@ice.mpg.de and kgroten@ice.mpg.de

bacterial and fungal species which function as biocontrol agents (Compant *et al.* 2005; Lugtenberg & Kamilova 2009; Santhanam *et al.* 2015b). For these interactions, many host and environmental factors affecting the colonization pattern are known. A number of studies showed the influence of soil characteristics, seasonal changes and genotypes on root microbial communities (Costa *et al.* 2006; Doornbos *et al.* 2011; Bulgarelli *et al.* 2012a; Lundberg *et al.* 2012; Peiffer *et al.* 2013; Philippot *et al.* 2013; Schlaeppi *et al.* 2013; Schreiter *et al.* 2014; Wagner *et al.* 2014; Coleman-Derr *et al.* 2016), but for the majority of root colonizing microbes, it remains largely unknown which host-derived factors favour colonization of particular microbial taxa under natural conditions, and whether colonization is initiated by seedborne microbes. For several crop plants, the seedborne microbiome is known to play a crucial role in seed germination and establishment under adverse conditions and in the early stages of plant development (Hardoim *et al.* 2011, 2012; Truyens *et al.* 2015), but our understanding of these processes in native plants remains scarce.

Host-derived factors which may affect the plant's microbial communities can also be induced or altered by environmental conditions. UVB irradiation (280–320 nm) is an important part of sunlight, and its intensities vary depending on the region and time of the day. Previous studies showed that UVB radiation has various effects on plants including damage to DNA, alterations in transpiration and photosynthesis, changes in growth, development and morphology, and rearrangement of secondary metabolites (Davidson & Robson 1986; Caldwell *et al.* 1994, 2007; Mazza *et al.* 1999; Ruhland *et al.* 2005; Nawkar *et al.* 2013; Jenkins 2014; Kataria *et al.* 2014).

In plants, UVB is perceived by UV RESISTANCE LOCUS 8 (UVR8), a photoreceptor specific for UVB radiation (Rizzini *et al.* 2011), and *A. thaliana* uvr8 mutants are highly susceptible to the damage caused by high UVB radiation (Brown *et al.* 2005). Interestingly, *UVR8* is not only expressed in leaf and stem tissue but also in roots (Rizzini *et al.* 2011), indicating that the root system is capable of responding to UV light (Kutschera & Briggs 2012). UVR8 regulates the expression of chalcone synthase (CHS), a key biosynthetic enzyme of phenols and flavonoids. These aromatic compounds strongly absorb UVB light and hence can function as sunscreens that protect cells from damage (Reuber *et al.* 1993; Mazza *et al.* 1999, 2000; Izaguirre *et al.* 2007). Flavonoids also act as chemoattractant for *Rhizobia,* nitrogen-fixing bacteria that form root nodules on legumes (Hassan & Mathesius 2012). UVB-exposed plants also tend to be more resistant to attack from herbivores (Tilbrook *et al.* 2013), and in *A. thaliana,* UVB exposure confers cross-resistance to the fungal necrotrophic pathogen *Botrytis cinerea* through increases in sinapate accumulation, a phenolic compound whose biosynthesis is regulated by UVR8 (Demkura & Ballaré 2012). UVB radiation was also found to change the composition of the culturable bacterial community of field-grown peanut leaves (Jacobs & Sundin 2001). Although UVB-induced changes in the microbiome of above-ground tissues of plants have been shown, the effect of UVB on the root microbiome is unexplored and it remains unknown whether and how recruitment of root bacteria is related to the perception of UVB by *UVR8* and its downstream responses that include the elicitation of CHS.

Coyote tobacco (*Nicotiana attenuata)* germinates from long-lived seed banks in the typically nitrogen-rich soils of the postfire environment (Lynds & Baldwin 1998; Preston & Baldwin 1999; Baldwin 2001). The longevity of its seeds makes this species particularly interesting for the characterization of the seedborne microbiome communities. The natural environment of *N. attenuata* plants, the Great Basin Desert, Utah, USA, is further characterized by high light conditions and strong UVB irradiance. The importance of UVB for *N. attenuata's* herbivory defence has been demonstrated – UVB radiation along with 17-hydroxygeranyllinalool diterpene glycosides provides resistance against mirid attack under field conditions (Dinh *et al.* 2013). Both culture-dependent and culture-independent approaches have been employed to study the microbiomes of *N. attenuata* wild-type plants and isogenic lines silenced in phytohormone and mycorrhizal signalling pathways growing in a field plot (Long *et al.* 2010; Santhanam *et al.* 2014; Groten *et al.* 2015). The studies revealed that the microbiomes of plants grown on the same field plot were sufficiently variable to mask any effects of the loss of jasmonate and mycorrhizal signalling pathways from the host (Santhanam *et al.* 2014; Groten *et al.* 2015), but the loss of ethylene perception had discernible effects (Long *et al.* 2010). In contrast, strong differences were observed between the microbiomes of roots and shoots (Santhanam *et al.* 2014, 2015a).

The aim of this study was to investigate several factors, which may alter the structure of the root microbiome of *N. attenuata* plants. Based on a cultivation-dependent and cultivation-independent approach using seeds from different native populations, we show that *N. attenuata* seeds do not harbour a seedborne microbiome. The results of the pyrosequencing-derived bacterial and fungal diversity revealed that location only has a minor effect on microbial community composition. However, the UV-resistant genus *Deinococcus* was consistently highly abundant in *N. attenuata* roots in all natural populations. To further investigate whether UV-B perception and response influenced root colonization by native *Deinococcus* isolates, we conducted a microcosm experiment using a synthetic bacterial community consisting of four native strains isolated from the field to test the hypothesis that the plant's response to UVB radiation, its perception (*UVR8*) and response (*CHAL*) influence the root colonization.

Materials and methods

Sample collection

Nicotiana attenuata plants were collected in 2013 from five different locations in the Great Basin Desert Utah, USA: Burn (N 37.3332 W 113.9388; a.s.l.1337 m), Pahcoon Spring (N 37.2381 W 113.8284; a.s.l. 1125 m), Wash (N 37.1396 W 114.0278; a.s.l. 839 m), Gate (N 37.1428 W 114.0224; a.s.l. 845 m) and Lytle-field plot (N 37.1463 W 114.0198; a.s.l. 844 m) (Fig. 1A). For plants of the Lytle-field plot, wild-type (WT) *Nicotiana attenuata* Torr. Ex S. Watson seeds of the 31st inbred generation were surface-sterilized and germinated on Gamborg's B5 plates (Duchefa) as previously described (Krügel *et al.* 2002) and transferred to individual Jiffy pots and planted in a field plot located at the Lytle Ranch Preserve, Utah, USA, as described in Diezel *et al.* (2009). For the other four locations, plants were naturally grown and not privately owned or protected in any way, so no special permits were required to collect the samples. We harvested nine plants from the Gate (G), Wash (W), Lytle (L) locations and three plants from Burn (B) and Pahcoon Spring (P). Except for some plants of the Wash population, all plants were in the elongating stage of growth which marks the transition from vegetative to reproductive growth for this annual plant. Differences in the numbers of plants harvested among sites were due to limited availability of plants in the native populations. Root samples were harvested, transported on ice to the field station, washed in running tap water to remove soil particles, dried in paper bags and transported to the laboratory, MPI-CE, Jena, Germany. Bulk soils were collected, adjacent (~1 m) to the sampled plants. Total P, Ca and K were determined by ICP-MS [ICP-Atomic Emission Spectrometer 'Optima 3300 DV' (PerkinElmer)] after microwave-based digestion, and total C and N were determined by combustion (Vario EL II"-Elementar Analysensysteme GmbH, Hanau). Chemical properties of soil samples were measured at the Max Planck Institute for Biogeochemistry as described (Quesada *et al.* 2010). For the seed microbiome analysis, seeds from different native populations were used mainly from a previous study (Kallenbach *et al.* 2012), as well as from different samplings in the plant's native habitat during different years. A list is provided in Table S1 (Supporting information). For the culture-dependent approach, surface-sterilized seeds according to the seed germination protocol of Krügel *et al.* (2002) and crushed seed extracts were plated on nutrient (Sigma) and R2A agar (Roth) and incubated for 7 days at 28 °C. Seeds (about 100) were crushed under sterile conditions with a sterile pestle and mortar and 300 µL of sterile distilled water.

DNA extraction, sample pooling and PCR amplification

Total DNA was extracted from three root and soil samples from each location using the FastDNA™ Spin kit for soil (MP biomedicals). For the G, W and L locations, nine roots were pooled to create three samples; thus, in total, 30 samples (15 from each compartment) were used. The concentration of DNA was determined by a NanoDrop ND 1000 spectrophotometer (Thermo Scientific, Wilmington, USA) and diluted to a working concentration of 30 ng/µL. For 454 pyrosequencing, samples were sent to MR.DNA (http://mrdnalab.com/), Texas, USA. Variable regions from V5 to V9 of the bacterial 16S rDNA gene were amplified by the following primer sets: 799F-1394R: ACCMGGATTAGA TACCCKG-ACGGGCGGTGTGRTC (Chelius & Triplett 2001). Based on our previous research (Santhanam *et al.* 2014), we selected primer set 799F-1394R, because it excludes the amplification of chloroplast and cyanobacteria nucleotides. For fungal community analysis, primers ITS1F (CTTGGTCATTTAGAGGAAGTAA, Gardes & Bruns 1993) and ITS4 (TCCTCCGCTTATTGATATGC, White *et al.* 1990) were used. A single-step 30-cycle PCR using HotStarTaq Plus Master Mix Kit (Qiagen, Valencia, CA, USA) was used under the following conditions: 94 °C for 3 min, followed by 28 cycles of 94 °C for 30 s; 53 °C for 40 s and 72 °C for 1 min after which a final elongation step at 72 °C for 5 min was performed. After PCR, all amplicon products from the different samples were mixed in equal concentrations and purified using the Agencourt Ampure beads (Agencourt Bioscience Corporation, MA, USA). Samples were sequenced with Roche 454 FLX titanium and corresponding reagents following the manufacturer's instructions.

For the seedborne microbiome analysis, DNA was extracted from surface-sterilized seeds also with FastDNA™ Spin kit for soil, and PCR was performed using the same primers as mentioned above. PCR amplification was performed in a 20 µL final volume of ReadymixTaq PCR mix (Sigma Aldrich) containing 1 µL of template DNA and 300 nM for each primer. Annealing temperature for the bacterial primers was 55 and 54 °C for the fungal primer pair. 40 cycles were performed to ensure that also putative small amounts of microbial

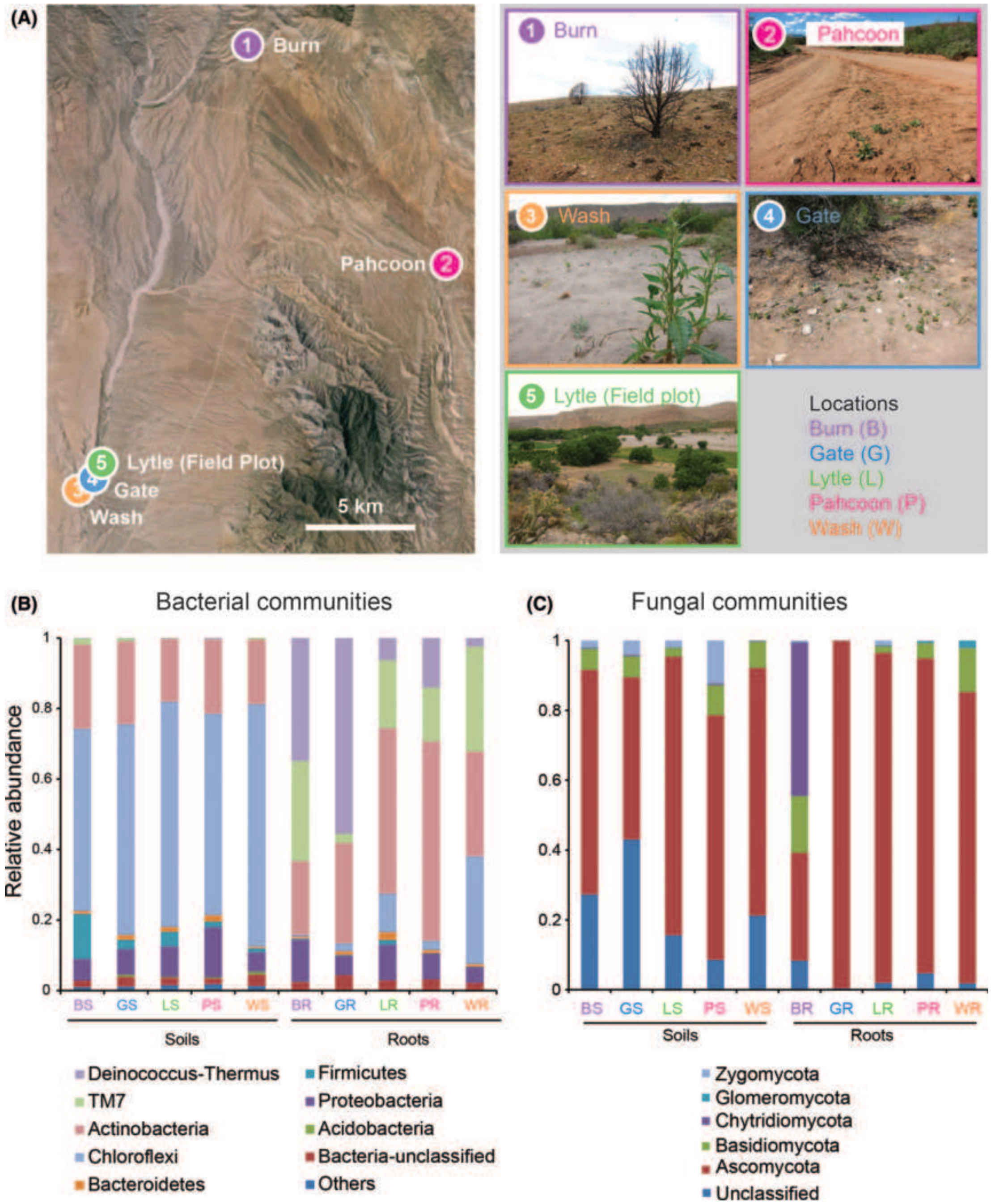

Fig. 1 Native-grown *N. attenuata* plant roots recruit distinct microbial communities compared to soils. (A) Location and pictures of the five different *N. attenuata* native populations used in this study in the Great Basin Desert Utah, USA. *N. attenuata* root (R) and soil (S) samples were collected from these locations. Relative abundance of root and soil bacterial (B) and fungal (C) communities at the phylum level. DNA was extracted from roots and soils. (B) for bacterial communities the V5–V9 variable region of 16S rDNA was amplified, sequenced by 454 pyrosequencing and analysed using the QIIME platform. Only the most abundant bacterial phyla are shown; the remaining phyla represent <1% of relative abundance. They include Armatimonadetes, Chlamydiae, Chlorobi, Cyanobacteria, FBP, Fibrobacteres, Gemmatimonadetes, Nitrospirae, OP3, Planctomycetes, SBR1093, Tenericutes, Verrucomicrobia and Acidobacteria. (C) For analysis of the fungal communities, the ITS1–4 regions were sequenced by 454 pyrosequencing. The phylum Ascomycota dominated the root and soil fungal communities. The fungal phyla present in soils and roots were not clearly distinct, and most phyla are present in both compartments. Ascomycota significantly differed among locations (L ratio= 31.23, $P < 0.0001$, pairwise Tukey, Burn:Lytle, t-ratio = −3.9, $P = 0.007$, Gate:Lytle, t-ratio = −3.1, $P = 0.03$). Each bar shows the average relative bacterial abundance of three biological replicates. Abbreviations – Burn (B), Gate (G), Lytle-field plot (L), Pahcoon (P) and Wash (W).

DNA are amplified. As additional controls, the solution used for surface sterilization, the washes and a part of the same batch of seeds were also plated on the same media, but no bacterial or fungal growth was observed in any of these controls.

Analysis of pyrosequencing data and statistical analysis

QIIME, PRIMER E software v.6 package (Clarke & Gorley 2006) and R version 3.1.1 were used for all statistical analysis. The QIIME software package was used to analyse the reads using default parameters for each step (Caporaso *et al.* 2010b). Sequences were removed if the average quality scored <25, lengths were shorter than 200 bp, excess of six bases homopolymer runs, primer mismatch and ambiguous bases. Most abundant sequences were taken as representative sequence for each cluster and aligned to the GREENGENES database, version 13_5 (McDonald *et al.* 2012), using PyNast algorithm with minimum per cent identity at 80% (Caporaso *et al.* 2010a). After alignment, USEARCH series of scripts were used to remove the chimer and noisy sequences followed by clustering of OTUs picking with 97% cut-offs (Edgar *et al.* 2011). Taxonomy was assigned using RDP classifier with a minimum support threshold at 80% (Wang *et al.* 2007). OTUs with the same taxonomy at phyla level were pooled for description of community. For further downstream analysis singletons, archaea and mitochondria were removed. Fungal reads were processed with default settings recommended by QIIME (http://qiime.org/tutorials/fungal_its_analysis.html), and chimeras were removed as mentioned above. We used Unite 12_11 files (http://unite.ut.ee) and pick_open_reference_otus.py script with default parameters to pick OTUs and assign taxonomy as recommended by Qiime http://nbviewer.jupyter.org/github/qiime/qiime/blob/master/examples/ipynb/Fungal-ITS-analysis.ipynb). Alignment to the ITS database was made with UNITE using the PyNast algorithm with a minimum per cent identity at 80% (Caporaso *et al.* 2010a). Library 'g plots' were used to construct Venn diagrams based on the 97% OTUs similarity. To find out the statistical significance of core OTUs, we conducted statistical comparisons with log2-transformed relative abundances (RA) per thousand values [log2(RA+1)] as described (Schlaeppi *et al.* 2013), with *P* values adjusted using the Bonferroni correction for multiple testing. Generalized linear squares (GLS) from library 'nmle' was used to assess the effect of 'soil' and 'root' on community composition among locations based on the phylum rank. R version 3.1.1 was used for ANOVA followed by Fisher's PLSD and Student's *t*-test for pairwise comparisons.

Identification of N. attenuata UVR8 and creation of NaUVR8 stably transformed lines

Comparing publicly available sequences at NCBI of *UVR8* from *Arabidopsis* and other closely related solanaceous species, for example *Solanum lycopersicum*, and *N. tabacum,* we identified homologs in *N. attenuata* using the *N. attenuata* 454 transcriptome database (Gase & Baldwin 2012). To generate *irUVR8* plants, we cloned a 319-bp fragment of *NaUVR8*gene as an inverted repeat construct into pRESC8 transformation vector containing a hygromycin (*hptII*) resistance gene as selection maker (Fig. S1A, Supporting information). *N. attenuata* plants were transformed as described in Krügel *et al.* (2002). Three independently transformed lines were screened according to Gase *et al.* (2011). All three lines met the requirements of homozygosity and showed silencing efficiencies of >95% (Fig. S1C, Supporting information). Homozygous transgenic lines were selected by screening of T_2 generation seeds that showed hygromycin resistance, and T-DNA insertions were confirmed by Southern blot hybridization, using genomic DNA from selected lines and ^{32}P-labelled PCR fragment of the *hptII* gene as hybridization probe (Fig. S1B, Supporting information). Quantitative real-time PCR (qPCR) was used to select the best silenced transgenic lines: *irUVR8*-160-5-6, 224-1-9 and 260-10-1, which showed more than 95% reduction in *NaUVR8* transcripts compared to EV plants.

For qPCR, total RNA was extracted from approximately 100 mg of frozen plant tissues with TRIzol reagent, followed by DNase-I treatment (Fermentas) according to the manufacturer's instructions. Remaining DNase was removed by phenol extraction and precipitated with addition of 3 M sodium acetate (pH 5.2) and pure ethanol. The cDNA was prepared from 1 μg of total RNA using Revert Aid^{TM} H Minus reverse transcriptase (Fermentas) and oligodT primer (Fermentas). Quantitative real-time PCR was conducted with synthesized cDNA using the core reagent kit for SYBR Green I (Eurogentec) and gene-specific primer pairs using Mx3005P PCR cycler (Stratagene). Relative gene expression was calculated from calibration curves obtained by analysis of dilution series of cDNA samples, and the values were normalized by the expression of the housekeeping gene, *NaEFα1* (*N. attenuata* elongation factor alpha 1). All reactions were performed using the following qPCR conditions: initial denaturation step of 95 °C for 30 s, followed by 40 cycles each of 95 °C for 30 s, 58 °C for 30 s and 72 °C for 1 min, followed by melting curve analysis of PCR products. The following primers were used: NaUVR8_For: 5′-AGGGGAGAGGATGGACAACT, NaUVR8_Rev: 5′-TGGAGTTTCCATGACCCAAT, Na_EF1a_For: 5′-CCACACTTCCCACATTGCTGTCA, Na_EF1a_Rev: 5′-CGCATGTCCCTCACAGC

AAA, Na_CHAL _FWD2 5′GCCTTTCAGATTGGAACT CG 3′, Na_CHAL _RVS2 5′ CAAGCCCTTCTTTTGCT GAG 3′.

Crossing irUVR8 and irCHAL

The cross between ir*UVR8* (260-10-1) and ir*CHAL* (283-1, previously described in Kessler *et al.* 2008) was created by hand pollination using ir*UVR8* and ir*CHAL* plants as a pollen donor and pollen acceptor, respectively, in the glasshouse. The hemizygote ir*UVR8* x ir*CHAL* plants showed reductions of ≈ 95% in *NaUVR8* and ≈75% in *NaCHAL* transcript accumulation compared to those of EV plants (Fig. S2, Supporting information).

Characterization of irUVR8 lines in the field

For field releases, empty vector (EV – WT, plants transformed with an empty vector construct, were used as controls) and ir*UVR8* line 260-10-1, one of the best silenced lines, were germinated, transferred to the field as described above. The transgenic seeds were imported and plants released under US Department of Agriculture Animal and Plant Health Inspection Service (APHIS) permit and notification numbers 12-320-103 m and 13-350-101r, respectively. Plant growth parameters (rosette diameter and stalk height) were measured every 5 days ($N = 15$), and net photosynthetic rates and stomatal conductances were determined using a LI-6400XT portable photosynthesis analysis system (Li-COR Bioscience, Lincoln, NE, USA) with 2000 μmol/m^2/s PAR and 400 μmolCO_2/m^2/s of reference CO_2 concentration. The 1st stalk leaf was used for all measurement, and values were generated from four size-matched undamaged, EV and ir*UVR8* plants growing on the field plot of the Lytle Ranch Preserve.

Isolation of Deinococcus

Seeds of the 31st inbred generation of *N. attenuata* WT were surface-sterilized and germinated as described above. Ten days after germination, seedlings were transferred to Teku pots containing native soil collected from five different locations from the Great Basin Desert, Utah, USA (see sample collection and Fig. 1). Native soils were diluted with sterile autoclaved sand (1:1). Plants were grown under glasshouse condition for 3 weeks, maintained at a day/night cycle of 16 h (26–28 °C)/8 h (22–24 °C), supplemented by 600-W or 400-W high-pressure sodium lamps (Philips Sun-T Agro), and 45–55% relative humidity. After 3 weeks, roots were harvested and gently washed with sterile water to remove soil, and roots were crushed for 3 min followed by inoculations of three different media: glucose–yeast extract, R2A and tryptone–yeast extract. Plates were incubated at 28 °C for 1 week, and pink-coloured colonies were picked from plates, subcultured and stored in 50% glycerol solution at −80 °C. Bacterial isolates were identified based on 16S rDNA gene sequencing as described in Santhanam *et al.* (2014). Three bacterial strains showed 100% (603 bp) similarity with the highly abundant core OTU12140, and strain D61 was used for further experiments.

Microcosm experiment

For the microcosm experiment with four different bacterial isolates representing four different phyla, seeds of *N. attenuata* WT (31st inbred generation) and of transgenic lines impaired in UVB perception (ir*UVR8*, A-12-260-10-1) and flavonoid biosynthesis (ir*CHAL*, A-06-283-1-1) (Kessler *et al.* 2008) and a cross of both (ir*CHAL*xir*UVR8*) were germinated as described above. Ten days after germination, seedlings were transferred to a Magenta™ vessel box (W×L×H; 77 ×77 × 97 mm, Sigma, GA-7, Germany) filled with sand (0.7–1.2 mm grain size, Raiffeisen, Germany) and 50 mL of Ferty B1 fertilizer (Planta Düngemittel, Regenstauf, Germany, http://www.plantafert.de/) and inoculated with a mixture of the four bacterial isolates by combining equal concentration of individual isolates (*Arthrobacter nitroguajacolicus*-E46 (Actinobacteria), *Pseudomonas frederiksbergensis*-A176 (Proteobacteria), *Bacillus mojavensis*-K1 (Firmicutes) isolated from field-grown roots from an earlier study (Santhanam *et al.* 2014) and *Deinococcus citri*-D61 from overnight-grown single cultures to obtain a working concentration of 10^6 CFU/mL. Seedlings were grown in a Voetsch growth chamber (22 °C, 65% humidity, 16-h light/8-h dark). Half of the plants were exposed to UVB (≈ 1.5 μmol/m^2/s, 290–315 nm) for 4 h per day from 10 AM to 2 PM. These time points were selected based on observations of UVB fluences in *N. attenuata*'s native habitat in May to June 2014 (Fig. S1D, Supporting information, UVB fluences of a representative day are shown, 21 May 2014). Thirty-six days after inoculation, roots were harvested and stored at −80 °C for quantification of bacterial communities by qPCR and to measure UV-absorbing phenolic compounds. Phenols were extracted in methanol:HCl (99:1) and the absorbance determined at 305 nm (A305) as described by Izaguirre *et al.* (2006).

Primer specificity and quantification of bacteria

Bacterial species-specific primers were designed using Primique software (Fredslund & Lange 2007). Specificity of primers was tested against bacterial isolates and plant DNA by PCR. The primer pair was considered to be specific if only a single PCR product was visible in an agarose gel in samples containing DNA of the respective species. PCR amplification was performed in a 20 μL final volume of ReadymixTaq PCR mix (Sigma Aldrich) containing 1 μL of template DNA (1 ng/μL) and 300 nM for each primer under the following PCR conditions: 95 °C for 1 min, followed by 35 cycles of denaturation at 95 °C for 60 s, annealing at 63 °C for 60 s and primer extension at 72 °C for 60 s, followed by a final extension at 72 °C for 10 min. The same conditions were used for qPCR. The quality of the PCR was examined by running an aliquot of the PCR product in 1.2% (w / v) agarose containing ethidium bromide.

For quantification of root bacterial colonization in the microcosm experiment, the same primers and procedures as described above were used for qPCR (Fig. S3, Supporting information). All samples were run in triplicates, and the average Ct values are reported. For the generation of standard curves, PCR products from four primers were diluted (10-fold serial dilutions $1–10^{-8}$ ng/μL) after measuring the PCR products using a Nanodrop ND1000 spectrophotometer (Thermo Scientific, Wilmington, USA). The PCR efficiency of all four reactions was between 95 and 105%, acceptable range of PCR efficiency 90–110% under MIQE guidelines (Bustin *et al*. 2009; Broeders *et al*. 2014). Based on the standard curves, absolute copy numbers of specific 16S rDNA templates were calculated as described by Lee *et al*. (2006, 2008). 16S rDNA gene copy numbers were normalized by number of operons from nearest neighbour strains (https://rrndb.umms.med.umich.edu/) (Stoddard *et al*. 2015) and log10 transformed. D61 and D78 share 100% similarity with *D. citri*, D71 and D80 with *D. depolymerans*. D79 and D63 are 96.6% similar to *D. daejeonensis*. qPCR products were purified and sequenced as described above.

Results

N. attenuata does not harbour a seedborne microbiome

To investigate the seedborne microbiome of *N. attenuata*, we used both culture-dependent and culture-independent approaches. After surface sterilization, none of the intact and crushed seeds showed any bacterial or fungal growth (Table S1, Supporting information), and the controls from the different washing steps after DCCS treatment were also negative; only the seeds of one bulk seed collection from the Apex mine burn in 1999 showed any evidence of bacterial growth from more than the 10 different seed collections tested from different years. Based on 16S rDNA sequencing, the only bacterium present in this 1999 collection was identified as *Curtobacterium flaccumfaciens*, a known seedborne pathogen (Camara *et al*. 2009). DNA was extracted from the same seeds as those used for the culture-dependent approach and subjected to PCR with the universal bacterial 799F-1394R and fungal ITS1F-ITS4R primers. No amplification was observed in any seed DNA, but only in the positive controls of bacterial and fungal DNA (Fig. S4, Supporting information). To verify whether, seed DNA inhibits the PCR, we used another bacterial primer pair (Primers 27F-1492R), which proceed a PCR product, but sequencing revealed that the reads belong to *N. attenuata's* chloroplast not bacterial DNA. Primer pair 27F and 1492R are well known to amplify chloroplast DNA (Cyanobacteria). Based on these results, we infer that *N. attenuata* does not harbour a seedborne microbiome and plants recruit microbial communities from the surrounding soil during germination and plant development.

Native root microbiomes are dominated by Actinobacteria, Deinococcus–Thermus and TM7 bacteria phyla and Ascomycota fungal phyla irrespective of locations

To investigate the recruitment of the *N. attenuata* root bacterial communities across native populations of plants, we sampled native-grown *N. attenuata* roots and bulk soil from five different locations at the Great Basin Desert, Utah, USA (Fig. 1A). The locations are a maximum of 35 km apart; hence, climatic conditions are reasonably similar among the locations. Based on the chemical properties of the soils, the Pearson correlation analysis indicates that Burn (B) and Pahcoon (P) soils are distinct from those from the Gate (G), Lytle (L) and Wash (W) populations (Fig. S5, Supporting information). The bacterial and fungal communities were determined based on barcoded 454 pyrosequencing of 16S rDNA and ITS, respectively, using the QIIME platform. Due to the field sampling in a remote area, this core community comprises rhizoplane and endosphere microbial communities.

For downstream analysis of bacterial communities, singletons, mitochondria and archaea were removed, and the number of sequences per sample rarified to 1310 reads (Fig. S6, Supporting information), which resulted in a total of 5122 OTUs from 22 taxa at the phyla level based on 97% similarity (Fig. 1B). Among these phyla, seven (Actinobacteria, Bacteroidetes, Chloroflexi, Proteobacteria, Firmicutes, Deinococcus–Thermus and TM7) were shared between roots and soils and strongly dominated the root and soil communities representing more than 98% of relative abundance, while 15 phyla representing <2% of the total relative abundance were only recovered from soils but not from roots.

The dominant phyla in the roots were Actinobacteria (36%), Deinococcus–Thermus (23%) and candidate division TM7 (19%), and these represented 78% of the total relative abundance (Fig. 1B). These dominant phyla were subjected to generalized least squares (GLS) to find out whether they are significantly enriched in roots compared to soils or whether they differ among the locations. Actinobacteria, Deinococcus–Thermus and TM7 phyla significantly differed between compartments – soils vs. roots (Fig. S7, Supporting information), but were independent of the locations. In contrast, the phylum Chloroflexi (Fig. 1A) was significantly more abundant in soils than in roots (Fig. S7, Supporting information, L ratio = 51.3, $P = < 0.0001$) and differed among locations (Chloroflexi-L ratio = 27.9, $P = < 0.0001$).

The alpha diversity parameters within samples, Shannon diversity (Shannon & Weaver 1964) and Margalef's species richness (Magurran 1991), were calculated based on the OTUs at 97% sequence similarity. For bacteria, both indices were significantly higher in soils compared to roots (Fig. 2A,B, ANOVA, Margalef-$F_{9,20} = 27.1$, $P = < 0.0001$, Shannon-$F_{9,20} = 13.9$, $P = < 0.0001$). The higher bacterial diversity in soils was mirrored by a larger number of unique OTUs in soils (2843 OTUs) than in roots (1283 OTUs); only 498 of the 5122 OTUs found in all samples were shared by both root and soil. The beta diversity among the samples was determined based on the Bray–Curtis dissimilarity matrix for the analysis of similarities (ANOSIM) and nonmetric multidimensional scaling ordination (NMDS). ANOSIM corroborated that root bacterial communities were significantly different from soils ($R = 0.87$, $P = 0.001$), but not for locations ($R = 0.07$, $P = 0.16$) and in NMDS plots, root and soil bacterial communities clustered completely separately. Soil bacterial communities did not show any pattern, while root bacterial communities tended to cluster by location without being clearly distinct (Fig. 2C). These results were further corroborated by phylogenetic weighted and unweighted UNIFRAC distance measurement (Fig. S8, Supporting information).

Fungal reads were rarified to 5500 reads and resulted in a total of 1546 OTUs based on the 97% similarity criteria. The OTUs corresponded to five phyla present in all root and soil samples: Ascomycota, Basidiomycota, Chytridiomycota, Glomeromycota and Zygomycota with a clear dominance of Ascomycota with more than 85% of the total relative abundance in roots except for one site, and 45–70% in soil (Fig. 1C). There was no significant difference among the enrichment of Ascomycota in soils vs. roots (Fig. 1, L ratio = 2.01, $P = 0.15$), but the abundance of Ascomycota significantly differed among locations (Fig. 1, L ratio = 31.23, $P = < 0.0001$).

In contrast to the results obtained for bacteria, alpha diversity indices of fungal communities, Shannon and Margalef species richness, differed significantly among the samples from the different populations (Fig. 2D, E; ANOVA, Shannon: $F_{9,20} = 4.7$, $P = 0.001$, Margalef: $F_{9,20} = 5.4$, $P = 0.0008$) without showing a clear influence from the compartment (roots vs. soils). However, Shannon diversity was lower for all root samples compared to soil. Beta diversity ANOSIM differed significantly among fungal communities of soils and roots ($R = 0.7$, $P = 0.001$), and also for locations ($R = 0.4$, $P = 0.001$, Table 1), and in NMDS plot based on the Bray–Curtis dissimilarity matrix, root samples clustered predominantly in the upper part of the plot while soil samples clustered in the lower part (Fig. 2F), without being fully separated.

In summary, native-grown *N. attenuata* roots specifically recruit a subset of the total bacterial communities, which were dominated by the phyla Actinobacteria, Deinococcus–Thermus and TM7. Fungal community diversity was higher among the samples, and location had a more pronounced effect on the community composition, even though Ascomycota clearly dominated all root and soil samples.

Core root bacterial and fungal communities of native-grown N. *attenuata roots*

To robustly analyse the influence of location on the root microbiome of native-grown *N. attenuata*, we further investigated at a lower taxonomic level which taxa are present in all root samples and whether taxa are unique to locations. We examined the OTUs at 97% similarity levels. 49 OTUs of a total of 1781 OTUs were shared among all root samples (Fig. 3A); this core community represented 45–78% of the total relative abundance and belonged to only six phyla (Deinococcus–Thermus, Actinobacteria, TM7, Chloroflexi, Proteobacteria and Bacteroidetes), including two phyla (Proteobacteria, Bacteroidetes) which constituted <9% of the total relative abundance. Among the 49 core OTUs, 23 OTUs differed significantly among the soil and root compartments (Fig. 3C, Table S2, Supporting information). Most of the significant OTUs belong to the phyla Deinococcus–Thermus and Actinobacteria, and at the family level to Deinococcaceae, Streptomycetaceae and Trueperaceae, while other taxa tended to be underrepresented (Table S2, Supporting information). Unique bacterial OTUs at each location varied from 6.1% (PR), 6.7% (WR), 7.4% (BR), 8.9% (GR) and 14.1% (LR) of total relative abundance in the roots (Fig. 3, Fig. S9A, Supporting information).

Of 701 fungal root OTUs, 434 OTUs were unique to locations ranging from 1 (GR) to 25% (LR) of total

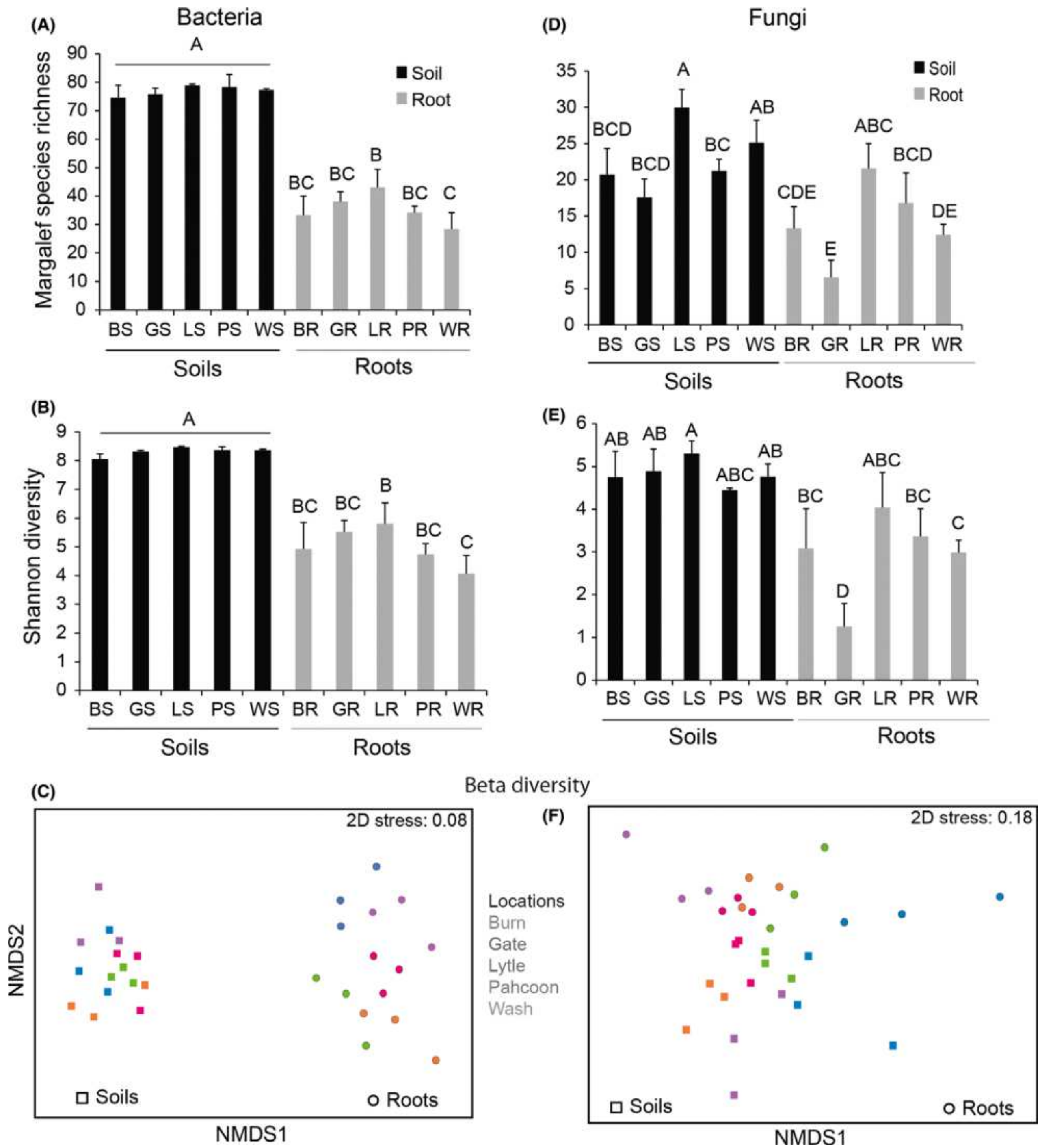

Fig. 2 Bacterial communities show a higher diversity in soils than in roots, and fungal communities differ among locations. The alpha diversity indices Margalef species richness (A) and Shannon (B) of rhizosphere and endosphere bacterial communities were significantly higher in soil compared to roots irrespective of locations. Whereas, for fungi alpha diversity indices, (D) Margalef species richness and (E) Shannon are not significantly different among soil and roots except for Gate location (GS & GR), (mean, ±SE, $N = 3$, different letters indicate significant differences, one-way ANOVA with Fisher's PLSD test; $P < 0.05$). (C–F) Nonparametric multidimensional scaling (NMDS) ordination based on the Bray–Curtis dissimilarity matrix for bacterial (C) and fungal root communities (F). Each dot corresponds to a different sample, the colour represents the location, and the shape indicates soil (□) and root (○). Abbreviations: S – soil, R – root; B – Burn, G – Gate, L – Lytle-field plot, P – Pahcoon, W – Wash.

Table 1 Pairwise ANOSIM of fungal communities at locations

Groups	*R*-statistic	*P*
Wash vs. Gate	0.5	0.002
Wash vs. Pachoon	0.2	0.06
Wash vs. Burn	0.35	0.01
Wash vs. Lytle	0.31	0.01
Gate vs. Pachoon	0.6	0.002
Gate vs. Burn	0.5	0.002
Gate vs. Lytle	0.5	0.002
Pachoon vs. Burn	0.36	0.006
Pachoon vs. Lytle	0.5	0.002
Burn vs. Lytle	0.4	0.002

relative abundance (Fig. 3B). 20 core OTUs belonging to the phylum Ascomycota – and at the family level Pleosporaceae – were found in all roots irrespective of locations. The core OTUs represented nearly 45 to 75% of the total relative abundance at three locations (LR, PR, WR) and 10 to 15% at two of the locations (BR, GR) (Fig. 3D). For both bacteria and fungi, the highest unique diversity was observed at the Lytle plot where the 31st inbred line was planted. Strong differences at the phylum level were observed for the fungal species found in the rhizosphere and endosphere of the roots: the phylum Basidiomycota was more abundant at Wash, Ascomycota at Lytle and Gate, Chytridiomycota at Burn site. This was also obvious for the fungal taxa unique to one location (Fig. 3B, Fig. S9B, Supporting information). From these results, we infer that the plants enrich a core bacterial and fungal community, but the site-specific root colonization by fungi is higher than it is for bacteria, and as a consequence, sampling location had a larger influence on the root fungal communities than on the bacterial communities.

Deinococcus–Thermus taxa are enriched in N. *attenuata roots and the isolation and culturing of Deinococcus citri*

Deinococcus was among the core OTUs whose abundance was significantly higher in roots than in soil. Interestingly, comparing the data from this and previous studies using the same species (Santhanam *et al.* 2014, 2015a; Groten *et al.* 2015), we found the phylum Deinococcus–Thermus in all root samples of native field-grown *N. attenuata* irrespective of plant developmental stages, and genotypes and field seasons; although relative abundance varied and ranged from 0.3 to 22%, except for Gate location with an abundance of about 50%.

Deinococcus–Thermus species are well known for their high resistance to UV and gamma radiation and their abilities to survive in harsh desert environments (Cox *et al.* 2010). These conditions characterize *N. attenuata*'s native habitat, the Great Basin Desert in Utah, USA, which regularly experiences UVB irradiance of ≈15 μmol/m^2/s (Fig. S1D, Supporting information). It is well known that a plant's chemical composition, as well as its root exudates, is influenced by UVB exposure (Caldwell *et al.* 2007; Hectors *et al.* 2014; Kaling *et al.* 2015). UVB exposure results in a dramatic increase in phenolic compounds (Mazza *et al.* 1999, 2000; Izaguirre *et al.* 2007), and the perception of UVB fluence is mediated by the UVR8 receptor (reviewed in Jenkins 2014). Therefore, we hypothesized that the specific enrichment of Deinococcus–Thermus in *N. attenuata* roots reflects the plant's response to UVB exposure. We further speculated that colonization is mediated by UVB perception through *NaUVR8* and its downstream response, the expression of Na*CHAL*, regulating the production of flavonoids which are known to protect plants from UV damage (Li *et al.* 1993; Agati & Tattini 2010). To test this hypothesis, the most abundant OTU from the phylum Deinococcus was OTU12140 which was highly abundant in all roots and shared 100% similarity with the *Deinococcus citri* NCCP-154^T type strain (Fig. 4A). We isolated a native *Deinococcus citri* strain by growing *N. attenuata* on the same native soils from which the root samples used in the pyrosequencing analysis were derived. Colonies which showed the characteristic purple colour were picked; sequencing analysis revealed that of 33 candidates, six isolates belonged to *Deinococcus* and two to *D. citri* (Fig. 4B, Table S3, Supporting information). Isolate *D. citri* D61 was selected for further experiments.

Generation and characterization of NaUVR8-silenced plants

As UVB is a crucial environmental factor for *N. attenuata* under natural conditions, we analysed the transcript levels of *NaUVR8* in 17 different tissues of native *N. attenuata* plants collected close to Pahcoon, and thus exposed to the same environmental conditions as the samples taken at one of the locations used for the microbiome analysis (Fig. 1). Interestingly, *NaUVR8* is not only expressed in above-ground tissues such as flower buds, leaves, and stalk, which are known to perceive and respond to light, but also in the transition part (root-to-shoot junction) and in below-ground tissues (primary and lateral roots, Fig. 5A). These results suggest that *NaUVR8* has yet unknown functions in below-ground tissues and might interact with bacterial microbial communities in the soils. For an in-depth functional analysis, we generated *NaUVR8*-silenced transgenic plants (ir*UVR8* plants, Fig. S3A, Supporting information). The silencing efficiency was >90%

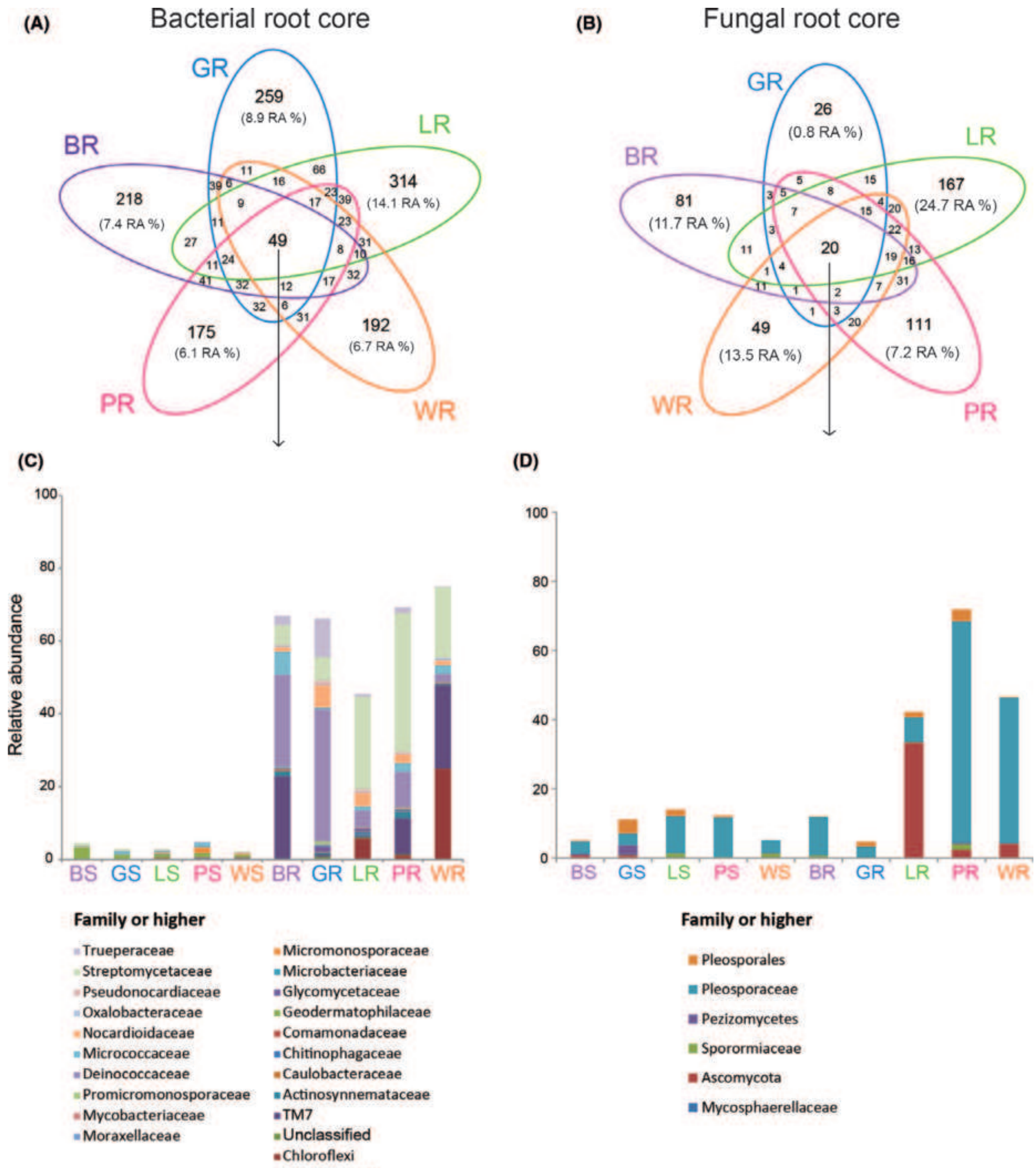

Fig. 3 The core bacterial and fungal root microbiota and their relative abundance. (A, B) Venn diagrams showing the distribution of bacterial and fungal measurable OTUs associated with *N. attenuata* roots by location. Core OTUs result from the intersection of the shared root bacterial and fungal OTUs identified at the five natural populations of *N. attenuata*. (A) *N. attenuata* harbours 49 core root OTUs of a total of 1781 OTUs identified in this study. Location had very little effect on shaping the root bacterial communities ANOSIM ($R = 0.07$, $P = 0.16$). Unique OTUs (97% similarity) constituted only 6.5–9.5% (except Lytle: LR-18.5%) of the total relative abundance of root bacterial communities. (C) The core root bacterial community constituted nearly 45–78% of total relative abundance. The core OTUs belong mainly to the dominant root phyla Actinobacteria, Deinococcus–Thermus and TM7, dominated at the family level by Trueperaceae, Deinococcaceae and Streptomycetidae. (D) The fungal core community of *N. attenuata* roots comprises 20 OTUs belonging to the phylum Ascomycota, and in particular to the families Pleosporales and Pleosporaceae; location influences the root fungal community. Locations significant effect on composition of the fungal root communities ANOSIM ($R = 0.4$, $P = 0.001$) and unique OTUs for each location range from 1 to 25%. Relative abundance of these OTUs is depicted for each location and for roots and soils and ranges from about 10–70%.

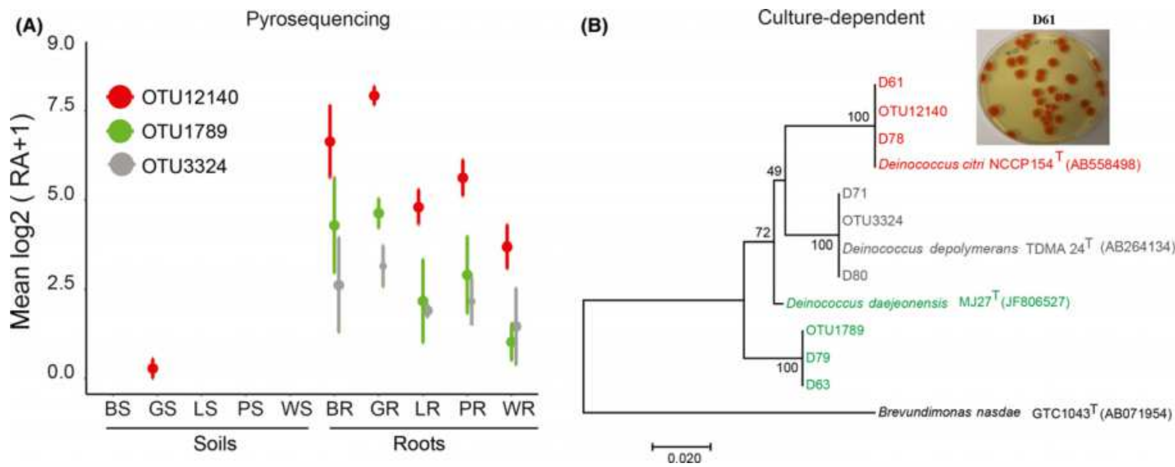

Fig. 4 *Deinococcus* was isolated from seedlings grown in native soil. (A) Within the phylum Deinococcus–Thermus, OTU 12140 is highly abundant in roots compared to other *Deinococcus* OTUs and shares 100% similarity with the type strain *Deinococcus citri* NCCP-154^T (Eztaxon database); $N = 3$. For abbreviations see Fig. 1. (B) Neighbour-joining tree based on V5–V8 hypervariable region of 16S rDNA gene depicts similarities among *Deinococcus* isolates from seedlings grown on soil samples retrieved from the five locations analysed in this study. In total, six *Deinococcus* strains were isolated and D61 and D78 isolates share 100% similarity with OTU 12140, D71 and D80 isolates share 100% similarity with OTU 3324 and D79, D63 isolates share 100% similarity with OTU 1789. For further analysis isolate D61-*D. citri* was selected because of its high abundance irrespective of all locations. Numbers at the nodes are percentage of bootstrap values based on 1000 resampled data sets. Bar: 0.02 substitutions per nucleotide position.

(Fig. S3C, Supporting information). The characterization of one of the best *NaUVR8*-silenced lines (ir*UVR8-260-10-1)* in the field at their native habitat, the Great Basin Desert, Utah, USA, which is characterized by high light conditions and strong UVB fluences (PAR max. ≈2000 μmol/m^2/s and UVB max. ≈15 μmol/m^2/s, Fig. S2D, Supporting information), revealed significantly lower net photosynthetic rates and also lower stomatal conductance than EV control plants (Fig. 5B). Photosynthetic rates correlated with growth parameters such as rosette diameter, and stalk diameter which were also slightly reduced in ir*UVR8* plants compared to EV (Fig. 5C, D).

UVB irradiance increases Deinococcus citri-D61 root colonization of WT host plants, but decreases colonization of plants impaired in the perception of and response to UVB

To evaluate the influence of UVB perception and downstream response on *Deinococcus* root colonization, we used WT plants and plants from the newly generated Na*UVR8*-silenced line, ir*CHAL* plants impaired in flavonoid biosynthesis (Kessler *et al*. 2008) and a cross of both (ir*UVR8*xir*CHAL*) to investigate not only the importance of UVB perception, but also to elucidate whether an active UVB response and protection system is relevant for *Deinococcus* colonization. To mimic natural conditions, plants were grown in microcosms under glasshouse (no-UVB) light conditions which were experimentally supplemented with UVB, using the same UVB fluence rate as measured in Utah (Fig. S2D, Supporting information). Seeds were inoculated with a synthetic bacterial community consisting of four bacterial isolates representing the four different phyla which are highly abundant in natural communities – *D. citri*-D61 (Deinococcus–Thermus), *Arthrobacter nitroguajacolicus*-E46 (Actinobacteria), *Pseudomonas frederiksbergensis*-A176 (Proteobacteria), *Bacillus mojavensis*-K1 (Firmicutes). The latter three species were selected based on their plant growth-promoting effects (Santhanam *et al.* 2014, 2015b). Species-specific primers were designed (Fig. S3, Supporting information) to determine the abundance of bacterial isolates by quantitative PCR (qPCR).

Isolate A176 (Proteobacteria) dominated the root community of *N. attenuata* followed by D61 (Deinococcus–Thermus), E46 (Actinobacteria) and K1 (Firmicutes) (Fig. 6, Fig. S10, Supporting information). In WT plants, UVB supplementation significantly increased (2.5-fold change) the colonization of *D. citri* compared to non-UVB supplemented plants (Fig. 6, ANOVA, $F_{7,32} = 6.9$, $P < 0.0001$), while root colonization of the other bacterial isolates was not significantly altered, although A176 and K1 colonization tended also to increase, but not that of E46 (Fig. S10, Supporting information, ANOVA, A176-$F_{7,32} = 1.8$, $P = 0.1$, E46-$F_{7,32} = 1.2$, $P = 0.3$, K1-$F_{7,32} = 1.8$, $P = 0.1$). Interestingly, the increase in *D. citri* D61 colonization correlated with higher amounts of

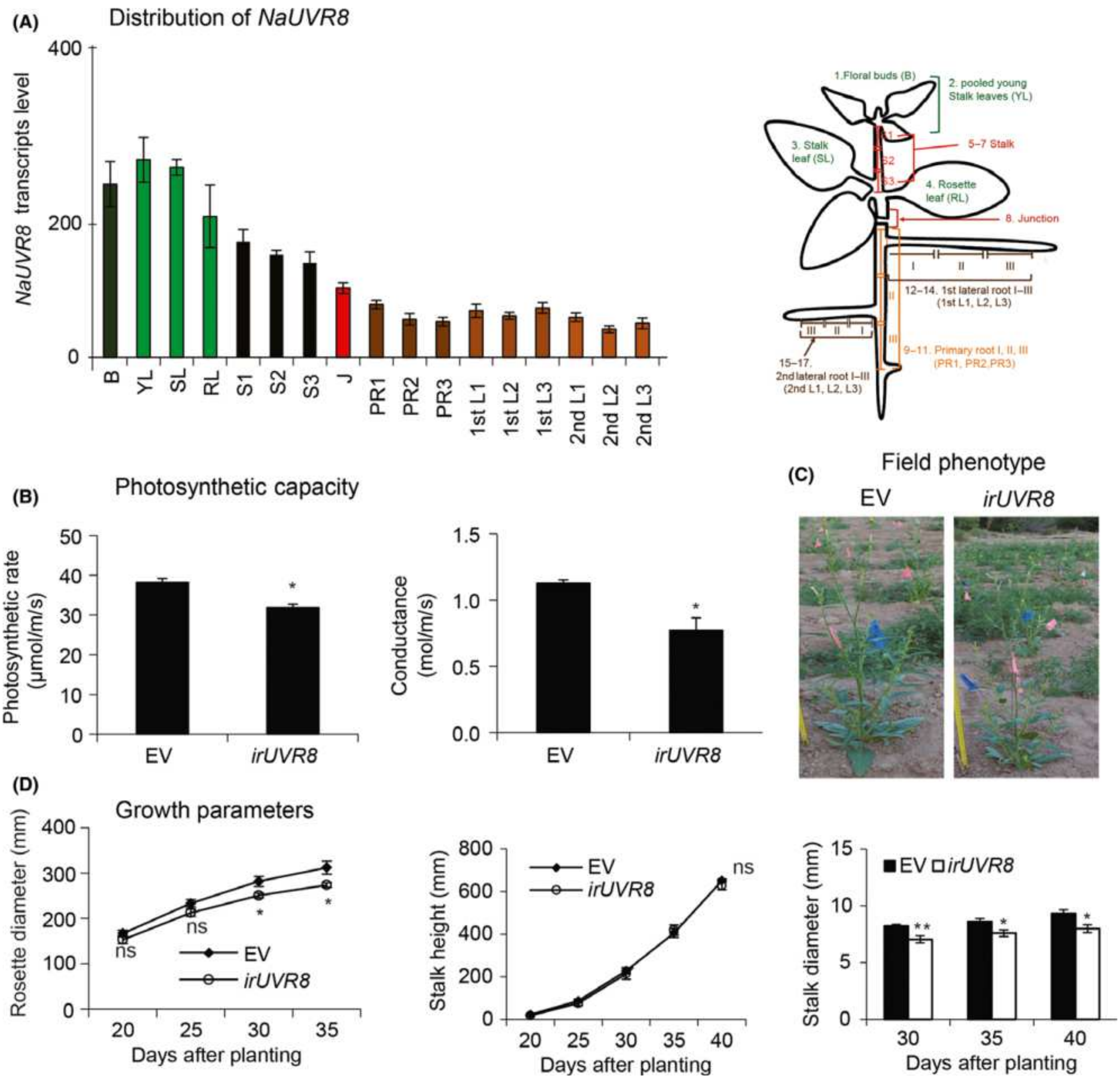

Fig. 5 *NaUVR8* transcript distributions in different tissues of native *N. attenuata* plants, and phenotype of *irUVR8* plants grown under field conditions. (A) 20 different tissues of native *N. attenuata* plants were collected in their native habitat, the Great Basin Desert, Utah, USA, and transcript abundance of *NaUVR8* in these tissues was determined by quantitative real-time PCR (qPCR). Bars indicate *EF1a*-normalized relative transcript abundances ($N = 7 \pm$ SE). (B) EV and ir*UVR8* plants were grown in the field (the Great Basin Desert, Utah, USA), and growth and development was monitored for 40 days (May to June 2014, $N = 15$, mean $\pm$ SE). ir*UVR8* plants showed a slight decrease in photosynthetic capacity compared to EV plants. Mean $\pm$ SE ($N = 4$) net photosynthetic rates and conductances in EV and *irUVR8* plants with the following parameters: photosynthetically active radiation = 2000 µmol/m/s, $CO_{2\ ref}$ = 400 μmol_{CO2}/m/s. (C, D) ir*UVR8* plants displayed smaller rosette and stalk diameters, but stalk heights were not significantly different from those of EV plants. Asterisks (B and D) indicate significant differences between EV and ir*UVR8* plants determined by Student's t-test at each measurement time (*$P \leq 0.05$, **$P \leq 0.01$).

phenolic compounds in roots under UVB exposure in WT (Fig. 6C), while, as expected, the ir*CHAL* and ir*UVR8* plants had significantly reduced levels of phenolic compounds after UVB exposure in a growth chamber (Fig. 6C, ANOVA, $F_{7,32} = 4.38$, $P = 0.001$).

In contrast to the response in WT plants, UVB supplementation decreased root colonization of *D. citri* D61 in the all three transgenic lines, ir*UVR8*, ir*CHAL* and ir*CHAL*xir*UVR8* (fold change 2.4, 2.1, 1.9, respectively, Fig. 6) compared to non-UVB-treated plants. From these

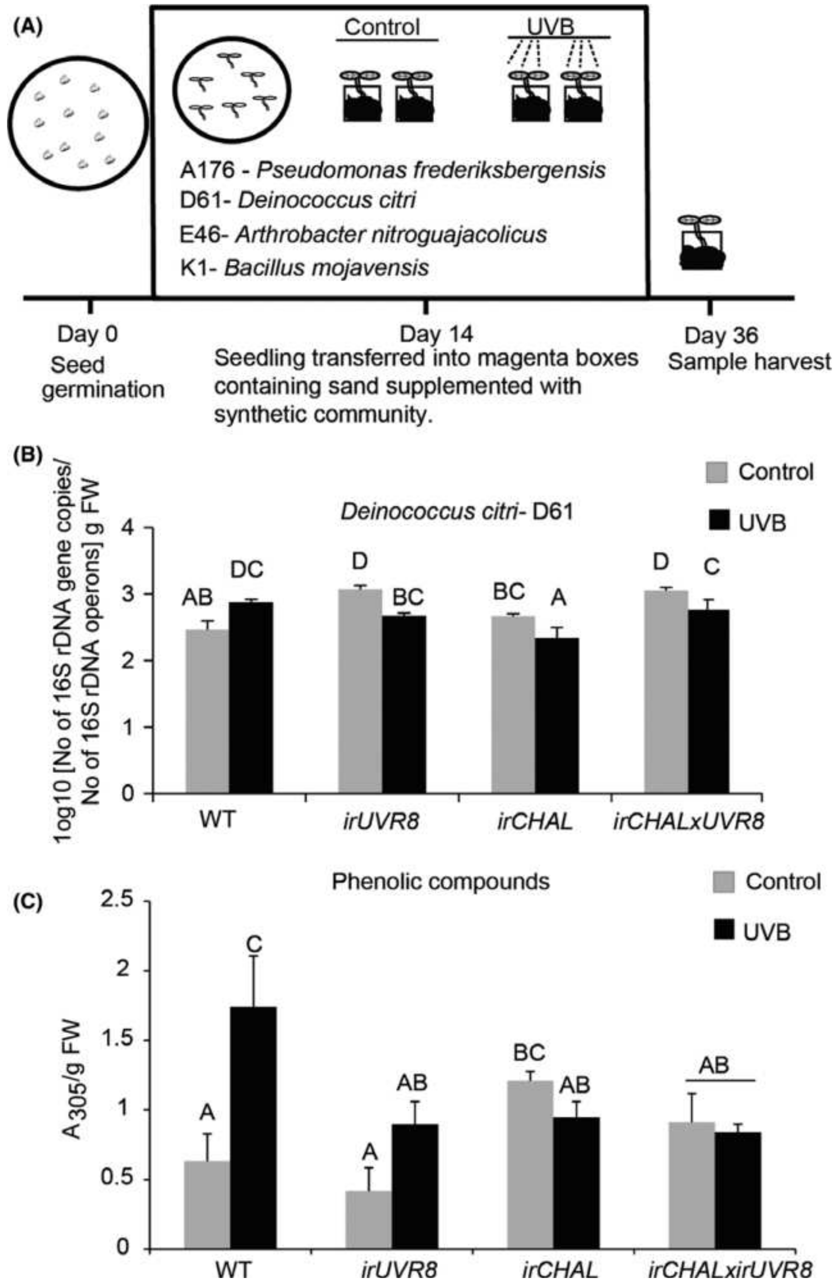

Fig. 6 UVB supplementation significantly increases the root colonization with *Deinococcus citri*-D61 and total phenolics in WT plants while colonization decreases and total phenolics remain unchanged in plants impaired in UVB perception and response. (A) Schematic representation of the experimental set-up in the growth chamber and list of bacterial species used for seedling inoculations. (B) Determination of bacterial abundance in the roots by qPCR with species-specific primers of the four bacterial species used in the experiment. With UVB supplementation, *Deinococcus citri*-D61 colonization significantly increased in wild type (WT), whereas colonization of *D. citri*-D61 decreased after UVB supplementation in plants silenced in the expression of the UV-receptor UVR8 (ir*UVR8*) and in the expression of a key biosynthesis enzyme of UVB inducible flavonoids (ir*CHAL*) and a cross of both (ir*CHALxirUVR8*). 16S rDNA gene copy numbers are normalized by number of operons from nearest neighbour *Deinococcus gobiensis* (rrnDB). (C) The same root samples were used to measure total phenolics at an absorbance of 305 nm, and phenolic compounds are significantly higher in UVB-exposed WT plants, but not in the transgenic lines. Mean ± SE, $N = 5$, different letters indicate significant differences, one-way ANOVA with Fisher's PLSD test; $P < 0.05$.

results, we infer that a plant's physiological responses to UVB exposure, which normally enhance root colonization, are altered when the perception and downstream signalling induced by UVB light are silenced, so that *D. citri* 61 colonization is impaired. *D. citri* D61 root colonization differed significantly among the genotypes ($F_{3,32}$ = 7.2, P = 0.0007), treatment (UVB vs. non-UVB, $F_{1,32}$ = 4.6, P = 0.04) and the interaction of both factors (genotypes*treatment, $F_{3,32}$ = 7.4, P = 0.0006). Thus, *NaUVR8* and *NaCHAL* probably play additional roles in root bacterial colonization, independent of their mediation of a plant's UVB responses.

In summary, these results indicate that UVB fluence rates and *N. attenuata*'s responses to UVB radiation, that include both perception of and responses to UVB fluence, are important factors affecting the recruitment of root bacterial communities.

Discussion

Plants maintain extensive close relationships with soil microbial communities, which can be affected by environmental and host-related factors, but how the host plant and its responses to environmental factors determine root colonization by fungal and bacterial communities remains for most taxa largely unknown. In a previous study, we investigated whether *N. attenuata's* capacity to produce jasmonic acid and calcium calmodulin protein kinase signalling affects the composition of the microbial communities in field-grown plants, but could not find major differences among the isogenic lines (Santhanam *et al.* 2014, 2015a; Groten *et al.* 2015), and we speculated that the local soil environment has a stronger effect on the plant's microbiome than the genotype. In this work, we expanded our analysis to the seedborne microbiome to evaluate whether a core group of microbes is transmitted to the offspring and serves as primary source for root colonization, and characterized the root microbiota of *N. attenuata* plants from different natural populations grown at different locations in their native habitat. We used this approach to make use of a native plant species which had not been subjected to agronomic selection, which may lead to a loss of many important survival traits (Degenhardt *et al.* 2009; Meyer *et al.* 2015), and to investigate plants exposed to the full spectrum of environmental factors in the field, as glasshouse-grown plants may fail to identify important abiotic and biotic factors relevant for microbiome recruitment and maintenance. In particular, the exposure to natural high UV-B frequencies cannot be readily mimicked in the glasshouse, but previous studies showed, for example, that bacterial diversity of the maize phyllosphere is controlled by several loci only under high UVB light exposure (Balint-Kurti *et al.* 2010).

We provide evidence that the ecological model plant *N. attenuata* does not harbour a seedborne microbiome (Fig. S4, Supporting information). This is contrary to findings of previous studies on maize showing a colonization of seeds with *Clostridium* and *Paenibacillus* species conserved across all *Zea* genotypes (Johnston-Monje & Raizada 2011). Similarly, the crop plants, rice and *Nicotiana tabacum*, harbour seedborne bacterial endophytes (Hardoim *et al.* 2008, 2011; Mastretta *et al.* 2009). The lack of a seedborne microbiome in *N. attenauata* suggests that the roots of this plant exclusively recruit bacterial and fungal communities from the soil soon after they germinate in native soils.

All roots investigated here harboured a core bacterial community which constituted 45-78% of relative abundance at the phylum level (Fig. 3A). The core community consisted of the phyla Actinobacteria, Deinococcus–Thermus, TM7, Proteobacteria, Bacteroidetes, and Chloroflexi. In an independent study in the same area and different year of sampling, these phyla – except of Chloroflexi – also dominated the root bacterial communities of the 31st inbred generation of *N. attenuata* WT grown on a field plot in the same area (Santhanam *et al.* 2014, 2015a; Groten *et al.* 2015), although the relative abundances differed among the studies. At a lower level of taxonomic resolution (OTUs; 97% similarity), individual OTUs represent <3% of relative abundance in all samples, while 49 core OTUs represented 45 to 78% of the relative abundance per sample. Thus, the remaining OTUs contribute to 22-55% of the total relative abundance, and host genotypes and location were not significant factors affecting bacterial community composition. This similarity could result from the relatively close proximity of the sampled populations and hence reflect similar climates, and rather than the small differences in soil conditions, altitude and population structures and likely high metabolic and genetic variability commonly found among plants growing in the same population (Kallenbach *et al.* 2012; Li *et al.* 2015, 2016). These results are consistent with those found from native Agave and Cacti, two perennial genera belonging to the CAM plants – which are adapted to a similar environment as *N. attenuata* – in which bacterial communities were also mainly influenced by plant compartment, while biogeography only had a minor effect (Coleman-Derr *et al.* 2016; Fonseca-García *et al.* 2016). Furthermore, different *Arabidopsis* genotypes grown on two different soil types in the glasshouse and a field study with 27 maize lines also showed that overall, bacterial communities among genotypes did not differ significantly and genotypes had a limited effect on shaping the root bacterial communities (Lundberg *et al.* 2012; Peiffer *et al.* 2013; Schlaeppi *et al.* 2013; Wagner *et al.* 2016).

In contrast to bacterial communities, location had an effect on fungal colonization of roots. Site-specific unique OTUs were enriched in roots (Fig. S9, Supporting information, Fig. 3), and soil and root communities did not clearly cluster separately as bacterial communities did (Fig. 2). Hence, the influence of location seems to be more important for fungi than for bacteria. This inference is further supported by differences in alpha diversity which we observed among individual locations and by the lower number of shared fungal OTUs, indicating that plants recruit fungi less specifically. In agreement with these results, biogeography and soil type had a strong effect on fungal communities in several other studies with native perennials such as of *Populus deltoides* (Shakya *et al.* 2013), Agave species (Coleman-Derr *et al.* 2016) and Cacti (Fonseca-García *et al.* 2016). Further research is needed to reveal whether the less specific enrichment of fungal rhizosphere and endosphere species depends more on the host genotype or location. Interestingly, the inbred line grown on the Lytle-field plot showed the largest amount of unique OTUs compared to other sites. This might be a treatment effect, because in contrast to the native populations, these plants were grown in their native habitat, but had been germinated on sterile plates; hence, these plants were not able to recruit a microbiome until 35 days after germination when they were transferred to native soil. This significant delay in the recruitment process may have led to higher colonization rates by taxa present in the surrounding soil.

In *N. attenuata*, the phylum Ascomycota dominated the fungal communities with more than 85% of total relative abundance in all roots (Fig. 1). At the family level, Pleosporaceae showed the highest abundance in the roots within the phylum Ascomycota. The high affinity of the phylum Ascomycota to different plant species on different soils may reflect their beneficial effects on plants. Among the 20 core OTUs in *N. attenuata* roots, a Blast search revealed highest similarity of two OTUs to *Epicoccum* and *Preussia*; both of these genera are described in literature to produce antifungal compounds (Fávaro *et al.* 2012; Mapperson *et al.* 2014). Interestingly, *Preussia* is among the most prominent fungal endophytes in above-ground tissues of nonsucculent desert plants (Massimo *et al.* 2015), while in the succulent Cactus species *Opuntia robusta* Prathoda was dominant (Fonseca-García *et al.* 2016). *Trichoderma*, well-known for its plant growth-promoting and biocontrol effects, was also present in some roots (Larkin & Fravel 2001). Based on these results, we infer that *N. attenuata* specifically recruits certain fungal communities and fungal OTUs that may help to protect itself from pathogen infection.

The characterization of the microbial communities present in roots provides valuable information on the specific enrichment of specific taxa, but only enables limited insights into the host-derived factors driving this process. Here, we further investigated the specific enrichment of the most abundant OTU 12140 in *N. attenuata* roots, corresponding to type strain *Deinococcus citri* NCCP-154^{T} and belonging to the phylum Deinococcus–Thermus. This phylum was found to be a consistent member of the plant's root microbiome in nature across year, locations and genotypes (Santhanam *et al.* 2014, 2015a; Groten *et al.* 2015), and OTU 12140 was almost exclusively found in roots, but not in the surrounding soil.

The phylum *Deinococcus* is known to include UV- and gamma radiation-resistant species (Makarova *et al.* 2001), and *P. ponderosa* plants as well as *N. attenuata* are exposed to high light and UV irradiation in their native habitats. UV light is known to induce the biosynthesis of flavonoids in leaves as protective sunscreens (Markstädter *et al.* 2001; Quattrocchio *et al.* 2006; Eichholz *et al.* 2012; Liu *et al.* 2012; Hectors *et al.* 2014), and very recently, it was shown in *Arabidopsis* that visible light can be transferred through stems to roots (Lee *et al.* 2016), which is consistent with our finding that the UVB-receptor UVR8 is expressed in all plant parts, including roots. So far it was unknown whether the plants' response to UVB exposure included changes in the structure of the root microbiome. By combining NGS with a functional-experimental analysis, we provide the first evidence that under UVB supplementation, *Deinococcus* colonization was significantly increased in WT plants (Fig. 6B), but not for the three other native bacterial species which were co-inoculated with *D. citri*. The results obtained with the three transgenic plants *irUVR8*, *irCHAL* and *irUVR8*x*irCHAL* revealed lower colonization rates after additional UVB supplementation compared to non-UVB-supplemented plants (Fig. 6B), demonstrating that the plant's responses to UVB are clearly relevant for root colonizing microbes.

We infer that UVB-induced metabolic changes (Fig. 6C), in particular those related to the activity of CHS, specifically enhance the *Deinococcus* root colonization. The secretion of flavonoids by roots serves as chemoattractant for the initiation of nodulation followed by bacterial *Rhizobium* colonization in legumes (Hassan & Mathesius 2012), and in WT plants, UVB exposure resulted in larger accumulations of phenolic compounds in the roots (Fig. 6C). Based on these findings, it is tempting to speculate that the UVB-induced flavonoid production may have increased *Deinococcus* colonization, although this relationship cannot be linear, as D61 colonization in ir*UVR8* controls was similar to that of WT plants with UVB exposure, even though amounts of phenolics were clearly different. Further experiments are required to understand the recruitment mechanisms in detail, and to rule out that *N. attenuata* not only provides a niche and protects *Deinococcus* from exposure to UV-light. Future studies will reveal whether *Deinococcus* might be specifically attracted by UVB-induced flavonoid production or whether CHS products function as a food source. Furthermore, *irUVR8* plants have lower net photosynthetic rates under natural light conditions, and hence may provide less sugar/nutrients for the bacteria (Fig. 5B); however, this effect would probably affect all bacteria used in the microcosm experiment, and not be specific for *Deinococcus*, as observed here.

In summary, we infer that *N. attenuata* seeds do not harbour an endophytic microbiome and that roots are exclusively colonized by bacteria and fungi as seeds germinate in native soils. Only a minor part of the root bacterial communities is sculpted by the environment, while more than 80% are specifically enriched in *N. attenuata* roots independent of the plant's locations. In contrast, root fungal communities are more strongly influenced by biogeography. One of the factors affecting the recruitment process is the plant's response to UVB light. A functional analysis mimicking natural conditions in a microcosm experiment revealed that under UVB supplementation, *Deinococcus* colonization increased in WT but not in the plants impaired in UVB perception (ir*UVR8*) and response (ir*CHAL*). These data suggest that UVB irradiation is an important factor not only for plants but also for their relationship with their bacterial partners. Additional work is required to fully understand the mechanism and metabolic processes responsible for increased *Deinococcus* colonization in nature under high PAR and high UVB irradiance.

Acknowledgements

We thank the Brigham Young University, Utah, USA, for use of their field station, the Lytle Ranch Preserve, D. Kessler and C. Diezel for field sample collections, E. McGale and Z. Ling for R scripts and help with the statistical analyses This study was funded by the Max Planck Society, by Advanced Grant 293926 from the European Research Council, by Human Frontier Science Programme RGP0002/2012 and by the Global Research Laboratory Programme Grant (2012055546) from the National Research Foundation of Korea, by a Max Planck-DST mobility grant to RK (2015-2018) and by a grant to VTL from the Leibniz Association.

References

Agati G, Tattini M (2010) Multiple functional roles of flavonoids in photoprotection. *New Phytologist*, **186**, 786–793.

Baldwin IT (2001) An ecologically motivated analysis of plant-herbivore interactions in native tobacco. *Plant Physiology*, **127**, 1449–1458.

Balint-Kurti P, Simmons SJ, Blum JE, Ballaré CL, Stapleton AE (2010) Maize leaf epiphytic bacteria diversity patterns are genetically correlated with resistance to fungal pathogen infection. *Molecular Plant-Microbe Interactions*, **23**, 473–484.

Bodenhausen N, Horton MW, Bergelson J (2013) Bacterial communities associated with the leaves and the roots of *Arabidopsis thaliana*. *PLoS One*, **8**, e56329.

Broeders S, Huber I, Grohmann L *et al*. (2014) Guidelines for validation of qualitative real-time PCR methods. *Trends in Food Science & Technology*, **37**, 115–126.

Brown BA, Cloix C, Jiang GH *et al*. (2005) A UV-B-specific signaling component orchestrates plant UV protection. *Proceedings of the National Academy of Sciences of the United States of America*, **102**, 18225–18230.

Bulgarelli D, Rott M, Schlaeppi K *et al*. (2012a) Revealing structure and assembly cues for *Arabidopsis* root-inhabiting bacterial microbiota. *Nature*, **488**, 91–95.

Bulgarelli D, Schlaeppi K, Spaepen S, Ver LvTE, Schulze-Lefert P (2012b) Structure and functions of the bacterial microbiota of plants. *Annual Review of Plant Biology*, **64**, 9.1–9.32.

Bustin SA, Benes V, Garson JA *et al*. (2009) The MIQE guidelines: minimum information for publication of quantitative real-time PCR experiments. *Clinical chemistry*, **55**, 611–622.

Caldwell MM, Flint SD, Searles PS (1994) Spectral balance and UV-B sensitivity of soybean: a field experiment. *Plant, Cell & Environment*, **17**, 267–276.

Caldwell MM, Bornman JF, Ballare CL, Flint SD, Kulandaivelu G (2007) Terrestrial ecosystems, increased solar ultraviolet radiation, and interactions with other climate change factors. *Photochemical & Photobiological Sciences*, **6**, 252–266.

Camara RC, Vigo SC, Maringoni AC (2009) Plant-to-seed transmission of *Curtobacterium flaccumfaciens pv. flaccumaciens* in a dry bean cultivar. *Journal of Plant Pathology*, **54**, 9–554.

Caporaso JG, Bittinger K, Bushman FD *et al*. (2010a) PyNAST: a flexible tool for aligning sequences to a template alignment. *Bioinformatics*, **26**, 266–267.

Caporaso JG, Kuczynski J, Stombaugh J *et al*. (2010b) QIIME allows analysis of high- throughput community sequencing data. *Nature Publishing Group*, **7**, 335–336.

Chelius MK, Triplett EW (2001) The diversity of archaea and bacteria. *Microbial Ecology*, **41**, 252–263.

Clarke KR, Gorley RN (2006) *PRIMER v6: User Manual/Tutorial*. PRIMER-E, Plymouth, UK.

Coleman-Derr D, Desgarennes D, Fonseca-Garcia C *et al*. (2016) Plant compartment and biogeography affect microbiome composition in cultivated and native *Agave* species. *New Phytologist*, **209**, 798–811.

Compant S, Duffy B, Nowak J, Clément C, Barka EA (2005) Use of plant growth-promoting bacteria for biocontrol of plant diseases: principles, mechanisms of action, and future prospects. *Applied and Environmental Microbiology*, **71**, 4951–4959.

Costa R, Götz M, Mrotzek N *et al*. (2006) Effects of site and plant species on rhizosphere community structure as revealed by molecular analysis of microbial guilds. *FEMS Microbiology Ecology*, **56**, 236 LP–249.

Cox MM, Keck JL, Battista JR (2010) Rising from the Ashes: DNA repair in *Deinococcus radiodurans* (SM Rosenberg, Ed,). *PLoS Genetics*, **6**, e1000815.

Davidson IA, Robson MJ (1986) Effect of contrasting patterns of nitrate application on the nitrate uptake, N2-fixation, nodulation and growth of white clover. *Annals of Botany*, **57**, 331–338.

Degenhardt J, Hiltpold I, Köllner TG *et al*. (2009) Restoring a maize root signal that attracts insect-killing nematodes to control a major pest. *Proceedings of the National Academy of Sciences*, **106**, 13213–13218.

Demkura PV, Ballaré CL (2012) UVR8 mediates UV-B-induced *Arabidopsis* defense responses against *Botrytis cinerea* by controlling sinapate accumulation. *Molecular Plant*, **5**, 642–652.

Diezel C, von DC, Gaquerel E, Baldwin IT (2009) Different lepidopteran elicitors account for cross-talk in herbivory-induced phytohormone signaling. *Plant Physiology*, **150**, 1576–1586.

Dinh ST, Galis I, Baldwin IT (2013) UVB radiation and 17-hydroxygeranyllinalool diterpene glycosides provide durable resistance against mirid *(Tupiocoris notatus)* attack in field-grown *Nicotiana attenuata* plants. *Plant, Cell & Environment*, **36**, 590–606.

Doornbos RF, Loon LC, Bakker PAHM (2011) Impact of root exudates and plant defense signaling on bacterial communities in the rhizosphere. *Agronomy for Sustainable Development*, **32**, 227–243.

Edgar RC, Haas BJ, Clemente JC, Quince C, Knight R (2011) UCHIME improves sensitivity and speed of chimera detection. *Bioinformatics*, **27**, 2194–2200.

Eichholz I, Rohn S, Gamm A *et al.* (2012) UV-B-mediated flavonoid synthesis in white asparagus *(Asparagus officinalis L.)*. *Food Research International*, **48**, 196–201.

Fávaro LdL, Sebastianes FdS, Araújo WL (2012) *Epicoccum nigrum* P16, a sugarcane endophyte, produces antifungal compounds and induces root growth (MR Liles, Ed,). *PLoS ONE*, **7**, e36826.

Fonseca-García C, Coleman-Derr D, Garrido E *et al.* (2016) The cacti microbiome: interplay between habitat-filtering and host-specificity. *Frontiers in Microbiology*, **7**, 150.

Fredslund J, Lange M (2007) Primique: automatic design of specific PCR primers for each sequence in a family. *BMC Bioinformatics*, **8**, 1–7.

Gardes M, Bruns TD (1993) ITS primers with enhanced specificity for basidiomycetes – application to the identification of mycorrhizae and rusts. *Molecular Ecology*, **2**, 113–118.

Gase K, Baldwin IT (2012) Transformational tools for next-generation plant ecology: manipulation of gene expression for the functional analysis of genes. *Plant Ecology & Diversity*, **5**, 485–490.

Gase K, Weinhold A, Bozorov T, Schuck S, Baldwin IT (2011) Efficient screening of transgenic plant lines for ecological research. *Molecular Ecology Resources*, **11**, 890–902.

Groten K, Nawaz A, Nguyen NHT, Santhanam R, Baldwin IT (2015) Silencing a key gene of the common symbiosis pathway in *Nicotiana attenuata* specifically impairs arbuscular mycorrhizal infection without influencing the root-associated microbiome or plant growth. *Plant, Cell & Environment*, **38**, 2398–2416.

Hacquard S, Kracher B, Hiruma K *et al.* (2016) Survival trade-offs in plant roots during colonization by closely related beneficial and pathogenic fungi. *Nature Communications*, **7**, 11362.

Hardoim PR, van OL, Elsas Jv (2008) Properties of bacterial endophytes and their proposed role in plant growth. *Trends in Microbiology*, **16**, 463–471.

Hardoim PR, Andreote FD, Reinhold-Hurek B *et al.* (2011) Rice root-associated bacteria: insights into community structures across 10 cultivars. *FEMS Microbiology Ecology*, **77**, 154–164.

Hardoim PR, Hardoim CCP, van OL, van Elsas JD (2012) Dynamics of seed-borne rice endophytes on early plant growth stages. *PLoS ONE*, **7**, e30438.

Hassan S, Mathesius U (2012) The role of flavonoids in root–rhizosphere signalling: opportunities and challenges for improving plant–microbe interactions. *Journal of Experimental Botany*, **63**, 3429–3444.

Hectors K, Van OS, Geuns J *et al.* (2014) Dynamic changes in plant secondary metabolites during UV acclimation in *Arabidopsis thaliana*. *Physiologia Plantarum*, **152**, 219–230.

Izaguirre MM, Mazza CA, Biondini M, Baldwin IT, Ballaré CL (2006) Remote sensing of future competitors: impacts on plant defenses. *Proceedings of the National Academy of Sciences*, **103**, 7170–7174.

Izaguirre MM, Mazza CA, SvatoŠ A, Baldwin IT, BallarÉ CL (2007) Solar ultraviolet-B radiation and insect herbivory trigger partially overlapping phenolic responses in *Nicotiana attenuata* and *Nicotiana longiflora*. *Annals of Botany*, **99**, 103–109.

Jacobs JL, Sundin GW (2001) Effect of solar UV-B radiation on a phyllosphere bacterial community. *Applied and Environmental Microbiology*, **67**, 5488–5496.

Jenkins GI (2014) The UV-B photoreceptor UVR8: from structure to physiology. *The Plant Cell*, **26**, 21–37.

Johnston-Monje D, Raizada MN (2011) Conservation and diversity of seed associated endophytes in Zea across boundaries of evolution, ethnography and ecology. *PLoS ONE*, **6**, e20396.

Kaling M, Kanawati B, Ghirardo A *et al.* (2015) UV-B mediated metabolic rearrangements in poplar revealed by non-targeted metabolomics. *Plant, Cell & Environment*, **38**, 892–904.

Kallenbach M, Bonaventure G, Gilardoni PA, Wissgott A, Baldwin IT (2012) *Empoasca* leafhoppers attack wild tobacco plants in a jasmonate-dependent manner and identify jasmonate mutants in natural populations. *Proceedings of the National Academy of Sciences of the United States of America*, **109**, E1548–E1557.

Kataria S, Jajoo A, Guruprasad KN (2014) Impact of increasing Ultraviolet-B (UV-B) radiation on photosynthetic processes. *Journal of Photochemistry and Photobiology B: Biology*, **137**, 55–66.

Kessler D, Gase K, Baldwin IT (2008) Field experiments with transformed plants reveal the sense of floral scents. *Science*, **321**, 1200–1202.

Krügel T, Lim M, Gase K, Halitschke R, Baldwin IT (2002) *Agrobacterium*-mediated transformation of *Nicotiana attenuata*, a model ecological expression system. *Chemoecology*, **12**, 177–183.

Kutschera U, Briggs WR (2012) Root phototropism: from dogma to the mechanism of blue light perception. *Planta*, **235**, 443–452.

Larkin RP, Fravel DR (2001) Efficacy of various fungal and bacterial biocontrol organisms for control of Fusarium wilt of tomato. *Plant Disease*, **82**, 1022–1028.

Lee C, Kim J, Shin SG, Hwang S (2006) Absolute and relative QPCR quantification of plasmid copy number in *Escherichia coli*. *Journal of Biotechnology*, **123**, 273–280.

Lee C, Lee S, Shin SG, Hwang S (2008) Real-time PCR determination of rRNA gene copy number: absolute and relative quantification assays with *Escherichia coli*. *Applied Microbiology and Biotechnology*, **78**, 371–376.

Lee H-J, Ha J-H, Kim S-G *et al.* (2016) Stem-piped light activates phytochrome B to trigger light responses in *Arabidopsis thaliana* roots. *Science Signaling*, **9**, ra106 LP–ra106.

Li J, Ou-Lee TM, Raba R, Amundson RG, Last RL (1993) *Arabidopsis* flavonoid mutants are hypersensitive to UV-B irradiation. *The Plant Cell*, **5**, 171–179.

Li D, Baldwin IT, Gaquerel E (2015) Navigating natural variation in herbivory-induced secondary metabolism in coyote tobacco populations using MS/MS structural analysis. *Proceedings of the National Academy of Sciences*, **112**, E4147–E4155.

Li D, Baldwin IT, Gaquerel E (2016) Beyond the Canon: within-plant and population-level heterogeneity in jasmonate signaling engaged by plant-insect interactions (D Gasperini, Ed,). *Plants*, **5**, 14.

Liu H, Li X, Xiao J, Wang S (2012) A convenient method for simultaneous quantification of multiple phytohormones and metabolites: application in study of rice-bacterium interaction. *Plant Methods*, **8**, 2.

Long HH, Sonntag DG, Schmidt DD, Baldwin IT (2010) The structure of the culturable root bacterial endophyte community of *Nicotiana attenuata* is organized by soil composition and host plant ethylene production and perception. *The New Phytologist*, **185**, 554–567.

Lugtenberg B, Kamilova F (2009) Plant-growth-promoting rhizobacteria. *Annual Review of Microbiology*, **63**, 541–556.

Lundberg DS, Lebeis SL, Paredes SH *et al.* (2012) Defining the core *Arabidopsis thaliana* root microbiome. *Nature*, **488**, 86–90.

Lynds G, Baldwin IT (1998) Fire, nitrogen, and defensive plasticity in *Nicotiana attenuata*. *Oecologia*, **115**, 531–540.

Magurran A (1991) *Ecological Diversity and its Measurement*. Chapman and Hall, London, UK.

Makarova KS, Aravind L, Wolf YI *et al.* (2001) Genome of the extremely radiation-resistant bacterium *Deinococcus radiodurans* viewed from the perspective of comparative genomics. *Microbiology and Molecular Biology Reviews*, **65**, 44–79.

Mapperson RR, Kotiw M, Davis RA, Dearnaley JDW (2014) The diversity and antimicrobial activity of *Preussia sp.* endophytes isolated from Australian dry rainforests. *Current Microbiology*, **68**, 30–37.

Markstädter C, Queck I, Baumeister J *et al.* (2001) Epidermal transmittance of leaves of Vicia faba for UV radiation as determined by two different methods. *Photosynthesis Research*, **67**, 17–25.

Massimo NC, Nandi DM, Arendt KR *et al.* (2015) Fungal endophytes in above-ground tissues of desert plants: infrequent in culture, but highly diverse and distinctive symbionts. *Microbial ecology*, **70**, 61–76.

Mastretta C, Taghavi S, van dLD *et al.* (2009) Endophytic bacteria from seeds of *Nicotiana tabacum* can reduce cadmium phytotoxicity. *International Journal of Phytoremediation*, **11**, 251–267.

Mazza CA, Battista D, Zima AM *et al.* (1999) The effects of solar ultraviolet-B radiation on the growth and yield of barley are accompanied by increased DNA damage and antioxidant responses. *Plant, Cell & Environment*, **22**, 61–70.

Mazza CA, Boccalandro HE, Giordano CV *et al.* (2000) Functional significance and induction by solar radiation of ultraviolet-absorbing sunscreens in field-grown soybean crops. *Plant Physiology*, **122**, 117–126.

McDonald D, Price MN, Goodrich J *et al.* (2012) An improved Greengenes taxonomy with explicit ranks for ecological and evolutionary analyses of bacteria and archaea. *The ISME journal*, **6**, 610–618.

Meyer RS, Whitaker BD, Little DP *et al.* (2015) Parallel reductions in phenolic constituents resulting from the domestication of eggplant. *Phytochemistry*, **115**, 194–206.

Nawkar GM, Maibam P, Park JH *et al.* (2013) UV-induced cell death in plants. *International Journal of Molecular Sciences*, **14**, 1608–1628.

Peiffer JA, Spor A, Koren O *et al.* (2013) Diversity and heritability of the maize rhizosphere microbiome under field conditions. *Proceedings of the National Academy of Sciences*, **110**, 6548–6553.

Philippot L, Raaijmakers JM, Lemanceau P, van dPW (2013) Going back to the roots: the microbial ecology of the rhizosphere. *Nat Rev Micro*, **11**, 789–799.

Preston CA, Baldwin IT (1999) Positive and negative signals regulate germination in the post-fire annual, *Nicotiana attenuta*. *Ecology*, **80**, 481–494.

Quattrocchio F, Baudry A, Lepiniec L, Grotewold E (2006) The regulation of flavonoid biosynthesis BT. In: *The Science of Flavonoids*. (ed Grotewold E), pp. 97–122. Springer, New York.

Quesada CA, Lloyd J, Schwarz M *et al.* (2010) Variations in chemical and physical properties of Amazon forest soils in relation to their genesis. *Biogeosciences*, **7**, 1515–1541.

Reuber S, Leitsch J, Krause GH, Weissenböck G (1993) Metabolic reduction of phenylpropanoid compounds in primary leaves of rye (*Secale cereale* L.) leads to increased UV-B sensitivity of photosynthesis. *Zeitschrift fuer Naturforschung. C, Biosciences*, **48**, 749–756.

Rizzini L, Favory J-J, Cloix C *et al.* (2011) Perception of UV-B by the *Arabidopsis* UVR8 Protein. *Science*, **332**, 103–106.

Ruhland CT, Xiong FS, Clark WD, Day TA (2005) The influence of ultraviolet-B radiation on growth, hydroxycinnamic acids and flavonoids of *Deschampsia antarctica* during springtime ozone depletion in Antarctica¶†. *Photochemistry and Photobiology*, **81**, 1086–1093.

Santhanam R, Groten K, Meldau DG, Baldwin IT (2014) Analysis of plant-bacteria interactions in their native habitat: bacterial communities associated with wild tobacco are independent of endogenous jasmonic acid levels and developmental stages. *PLoS ONE*, **9**, e94710.

Santhanam R, Baldwin IT, Groten K (2015a) In wild tobacco, *Nicotiana attenuata,* variation among bacterial communities of isogenic plants is mainly shaped by the local soil microbiota independently of the plants' capacity to produce jasmonic acid. *Communicative & Integrative Biology*, **8**, e1017160.

Santhanam R, Luu VT, Weinhold A *et al.* (2015b) Native root-associated bacteria rescue a plant from a sudden-wilt disease that emerged during continuous cropping. *Proceedings of the National Academy of Sciences*, **112**, E5013–E5020.

Schlaeppi K, Dombrowski N, Oter RG, Ver LvTE, Schulze-Lefert P (2013) Quantitative divergence of the bacterial root microbiota in *Arabidopsis thaliana* relatives. *Proceedings of the National Academy of Sciences*, **111**, 585–592.

Schreiter S, Ding G-C, Heuer H *et al.* (2014) Effect of the soil type on the microbiome in the rhizosphere of field-grown lettuce. *Frontiers in Microbiology*, **5**, 144.

Shakya M, Gottel N, Castro H *et al.* (2013) A multifactor analysis of fungal and bacterial community structure in the root microbiome of mature *Populus deltoides* trees. *PLoS ONE*, **8**, e76382.

Shannon CE, Weaver W (1964) *The Mathematica Theoryl of Communication*. The University of Illinois Press. Urbana, Illinois.

Stoddard SF, Smith BJ, Hein R, Roller BRK, Schmidt TM (2015) rrnDB: improved tools for interpreting rRNA gene abundance in bacteria and archaea and a new foundation for future development. *Nucleic Acids Research*, **43**, D593–D598.

Tilbrook K, Arongaus AB, Binkert M *et al.* (2013) The UVR8 UV-B photoreceptor: perception, signaling and response. *The Arabidopsis Book/American Society of Plant Biologists*, **11**, e0164.

Truyens S, Weyens N, Cuypers A, Vangronsveld J (2015) Bacterial seed endophytes: genera, vertical transmission and interaction with plants. *Environmental Microbiology Reports*, **7**, 40–50.

Wagner MR, Lundberg DS, Coleman-Derr D *et al.* (2014) Natural soil microbes alter flowering phenology and the intensity of selection on flowering time in a wild *Arabidopsis* relative. *Ecology Letters*, **17**, 717–726.

Wagner MR, Lundberg DS, del Rio TG *et al.* (2016) Host genotype and age shape the leaf and root microbiomes of a wild perennial plant. *Nature Communications*, **7**, 12151.

Wang Q, Garrity GM, Tiedje JM, Cole JR (2007) Naïve bayesian classifier for rapid assignment of rRNA sequences into the new bacterial taxonomy. *Applied and Environmental Microbiology*, **73**, 5261–5267.

White T, Bruns T, Lee S, Taylor J (1990) Amplification and direct sequencing of fungal ribosomal RNA genes for phylogenetics. In: *PCR Protocols: A Guide to Methods and Applications* (eds Innis M, Gelfand D, Shinsky J, White T), pp. 315–322. Academic Press, San Diego, California.

R.S. performed the experiments, analysed the data and drafted the manuscript. I.T.B. and K.G. revised the manuscript. Y.O. characterized the *irUVR8* line. R.K. performed the seed microbiome study. R.S., V.T.L., A.W., K.G. and I.T.B. conceived and designed the study.

Data accessibility

Sequencing data have been deposited in the European Nucleotide Archive-PRJEB13826.

Accession nos. of bacterial isolates are LT602895–LT602926.

NaUVR8 is available at DDBJ/EMBL/GenBank (gene ID KX094971).

Supporting information

Additional supporting information may be found in the online version of this article.

Fig. S1 *Nicotiana attenauata* seeds do not harbour bacterial and fungal microbiome.

Fig. S2 ir*UVR8* plants were transformed with an inverted repeat (ir) *NaUVR8* construct and UVB fluence under natural condition.

Fig. S3 Silencing efficiency of *irCHAL*, *irUVR8* lines and the cross of both lines.

Fig. S4 Bacterial species-specific primers.

Fig. S5 Chemical properties of the soils retrieved from five different locations at the Great Basin Desert, Utah, USA.

Fig. S6 Soil harbours higher bacterial and fungal diversity compared to roots.

Fig. S7 *N. attenuata* roots specifically recruit bacteria of the phyla Actinobacteria, Deinococcus–Thermus and TM7 from native soils.

Fig. S8 Archaeal reads were higher in soil compared to roots and phylogenetic measurement of bacterial beta diversity.

Fig. S9 Unique bacterial and fungal lineages at the different locations.

Fig. S10 Root bacterial colonization by strains A176, E46 and K1 is not influenced by UVB in WT, and also not in the plants impaired in UVB perception and responses.

Table S1 Seeds used for characterization of the seed microbiome by culture-dependent and –independent approaches, positive controls used for PCR, and results of the culture-dependent approach.

Table S2 23 of 49 core bacterial OTUs from *N. attenuata* significantly differed among soil and root samples.

Table S3 Bacterial isolates retrieved from roots of *Nicotiana attenuata*.